



**HAL**  
open science

## **Integrative analysis of proteomics and transcriptomics reveals endothelin receptor B as novel single target and identifies new combinatorial targets for multiple myeloma**

Margaux Lejeune, Murat Cem Köse, Mégane Jassin, Marie-Jia Gou, Amaury Herbet, Elodie Duray, Gaël Cobraiville, Jacques Foguene, Didier Boquet, André Gothot, et al.

### ► **To cite this version:**

Margaux Lejeune, Murat Cem Köse, Mégane Jassin, Marie-Jia Gou, Amaury Herbet, et al.. Integrative analysis of proteomics and transcriptomics reveals endothelin receptor B as novel single target and identifies new combinatorial targets for multiple myeloma. *HemaSphere*, 2023, 7 (7), pp.e901. 10.1097/HS9.0000000000000901 . hal-04485000

**HAL Id: hal-04485000**

**<https://hal.science/hal-04485000>**

Submitted on 1 Mar 2024

**HAL** is a multi-disciplinary open access archive for the deposit and dissemination of scientific research documents, whether they are published or not. The documents may come from teaching and research institutions in France or abroad, or from public or private research centers.

L'archive ouverte pluridisciplinaire **HAL**, est destinée au dépôt et à la diffusion de documents scientifiques de niveau recherche, publiés ou non, émanant des établissements d'enseignement et de recherche français ou étrangers, des laboratoires publics ou privés.

## Article

## Open Access

# Integrative Analysis of Proteomics and Transcriptomics Reveals Endothelin Receptor B as Novel Single Target and Identifies New Combinatorial Targets for Multiple Myeloma

Margaux Lejeune<sup>1,\*</sup>, Murat Cem Köse<sup>1,\*</sup>, Mégane Jassin<sup>1</sup>, Marie-Jia Gou<sup>2</sup>, Amaury Herbet<sup>3</sup>, Elodie Duray<sup>1</sup>, Gaël Cobraiville<sup>2</sup>, Jacques Foguene<sup>4</sup>, Didier Boquet<sup>3</sup>, André Gothot<sup>4</sup>, Yves Beguin<sup>1,5</sup>, Marianne Fillet<sup>2,\*\*</sup>, Jo Caers<sup>1,5,\*\*</sup>

**Correspondence:** Jo Caers (jo.caers@chuliege.be).

## ABSTRACT

Despite the recent introduction of next-generation immunotherapeutic agents, multiple myeloma (MM) remains incurable. New strategies targeting MM-specific antigens may result in a more effective therapy by preventing antigen escape, clonal evolution, and tumor resistance. In this work, we adapted an algorithm that integrates proteomic and transcriptomic results of myeloma cells to identify new antigens and possible antigen combinations. We performed cell surface proteomics on 6 myeloma cell lines based and combined these results with gene expression studies. Our algorithm identified 209 overexpressed surface proteins from which 23 proteins could be selected for combinatorial pairing. Flow cytometry analysis of 20 primary samples confirmed the expression of FCRL5, BCMA, and ICAM2 in all samples and IL6R, endothelin receptor B (ET<sub>B</sub>), and SLC05A1 in >60% of myeloma cases. Analyzing possible combinations, we found 6 combinatorial pairs that can target myeloma cells and avoid toxicity on other organs. In addition, our studies identified ET<sub>B</sub> as a tumor-associated antigen that is overexpressed on myeloma cells. This antigen can be targeted with a new monoclonal antibody RB49 that recognizes an epitope located in a region that becomes highly accessible after activation of ET<sub>B</sub> by its ligand. In conclusion, our algorithm identified several candidate antigens that can be used for either single-antigen targeting approaches or for combinatorial targeting in new immunotherapeutic approaches in MM.

## BACKGROUND

In the past decade, the survival of multiple myeloma (MM) patients has improved with the introduction of novel agents. The 5-year survival rates of a global myeloma population increased from 37% to 52% in a recent registry study, an increase that was mainly seen in young transplant-eligible patients.<sup>1</sup> With the introduction of the monoclonal anti-CD38 antibodies daratumumab and isatuximab, improvement of survival rates is likely to continue. When used in monotherapy, daratumumab showed clinical activity in 37% of refractory MM patients.<sup>2</sup> When combined with lenalidomide or bortezomib, the response rates increased to 92% and 85%, respectively.<sup>3,4</sup> Daratumumab is currently approved as the first-line treatment for both transplant-eligible and transplant-ineligible patients.<sup>5,6</sup>

Following monoclonal antibodies, more potent immunotherapeutic approaches are developed. Similar to other lymphoproliferative malignancies, chimeric antigen receptor (CAR) T-cell therapies and bispecific antibodies (BsAbs) have been introduced and successfully tested in early clinical trials.<sup>7,8</sup> For MM, these strategies targeted a limited set of antigens (B-cell maturation antigen [BCMA], G-protein coupled receptor family C group 5 member D [GPCR5D], and Fc receptor-like 5 [FCRL5]).<sup>9</sup> Nonetheless, malignant cells can escape immune recognition by employing a number of antigen-evasion strategies, including antigen mutation, downregulation of target antigens, and the selective survival of antigen-negative cell subpopulations.<sup>10</sup> Such immune escape has been well studied for patients relapsing after anti-BCMA CAR-T therapy or BsAbs. Homozygous deletions of chromosome 16p (where the *BCMA*

<sup>1</sup>Laboratory of Hematology, GIGA I3, University of Liège, Belgium

<sup>2</sup>Laboratory for the Analysis of Medicines, Center for Interdisciplinary Research on Medicines (CIRM), University of Liège, Belgium

<sup>3</sup>Université Paris-Saclay, CEA, Département Médicaments et Technologies pour la Santé (DMTS), SPI, Gif-sur-Yvette, France

<sup>4</sup>Department of Hematobiology and Immunohematology, CHU de Liège, Belgium

<sup>5</sup>Department of Hematology, CHU de Liège, Belgium

\*ML and MCK are co-first authors and have contributed equally to this work.

\*\*MF and JC are co-senior authors and have contributed equally to this work.

Ethical approval for this study was obtained from the institutional ethical board (Comité d'Éthique Hospitalo-Facultaire Universitaire de Liège) (EC2020/375).

Supplemental digital content is available for this article.

Copyright © 2023 the Author(s). Published by Wolters Kluwer Health, Inc. on behalf of the European Hematology Association. This is an open-access article distributed under the terms of the Creative Commons Attribution-Non Commercial-No Derivatives License 4.0 (CCBY-NC-ND), where it is permissible to download and share the work provided it is properly cited. The work cannot be changed in any way or used commercially without permission from the journal.

HemaSphere (2023) 7:7(e901).

<http://dx.doi.org/10.1097/HS9.0000000000000901>.

Received: December 22, 2022 / Accepted: April 25, 2023

gene is located) or a biallelic loss of BCMA have been reported in relapsing patients.<sup>11,12</sup> Hence, increasing the number of targeted antigens may result in a more effective therapy by preventing antigen escape and disease progression. This strategy is particularly relevant in patients with refractory disease, those relapsing after immunotherapy and/or rapid and aggressive disease progression.

On the contrary, immunotherapy should avoid activation toward antigens expressed on healthy tissues and cells (often termed on-target, off-tumor), particularly in patients with minimal bone marrow (BM) infiltration (eg, minimal residual disease), and thus highly selective and effective treatments are needed.<sup>13</sup> Tumor-specific targeting can also be increased by simultaneously targeting 2 antigens; even if neither antigen is expressed exclusively by the tumor, the tumor cells—but not healthy cells—are likely to express both antigens.<sup>14</sup> Figure 1 illustrates different forms of immunotherapy that are based on the combinatorial approaches such as CAR-T cells<sup>15</sup> and BsAbs.<sup>16,17</sup>

In this study, we aimed to identify optimal antigen pairs for selective MM cell targeting. These pairs were identified by combining proteomic and genomic results from myeloma and normal cell populations and their expression profiles were subsequently validated by flow cytometry (Figure 2A). We could propose different antigen combinations for immunotherapeutic approaches. Moreover, our algorithm revealed endothelin receptor B (ET<sub>B</sub>) as a potential new target for MM that is overexpressed compared with normal plasma cells and B-lymphocytes and absent on hematopoietic stem cells.

## METHODS

### Cell lines

Human MM cell lines KMS-12-BM, NCI-H929, MOLP-2, and RPMI-8226 were obtained from the German Collection of Microorganisms and Cell Cultures (Deutsche Sammlung von Mikroorganismen und Zellkulturen [DSMZ]; Braunschweig, Germany). U266, OPM-2, and LP-1 cell lines were obtained from H. Jernberg-Wiklund (Uppsala University, Uppsala, Sweden) and MM1.S was obtained from A. Bolomsky (Wilhelminen Cancer Research Institute, Vienna, Austria). LP-1 cells were cultured in Dulbecco's Modified Eagle's Medium (DMEM) (Lonza, Verviers, Belgium) supplemented with 10% fetal bovine serum (FBS; Sigma-Aldrich, St-Louis, MO), 2 mM L-glutamine (Lonza), and 100 U/mL penicillin-streptomycin (P/S; Lonza). RPMI-8226 cells, KMS-12-BM cells, U266 cells, MOLP-2 cells, OPM-2 cells, NCI-H929 cells, and MM1.S cells were cultured in Roswell Park Memorial Institute (RPMI 1640)

(Lonza) supplemented with 10% FBS, 2 mM L-glutamine, and 100 U/mL P/S. All cell lines were cultured at 37°C in 5% CO<sub>2</sub> humidity.

### Cell surface proteomics

Six myeloma cell lines, including OPM-2, LP-1, MOLP-2, U266, MM1.S, and KMS-12-BM, were selected for cell surface biotinylation and isolation. For this purpose, the Pierce Cell Surface Protein Isolation Kit (Thermo Fisher, Waltham, MA) was used for biotinylation, lysis, and isolation of labeled proteins. Three biological replicates of each above-mentioned cell lines were cultured in 75 cm<sup>2</sup> flasks to obtain 10<sup>7</sup> cells. For the biotinylation, cell lysis, and recovery of biotinylated proteins, we followed the instructions provided by the manufacturer. Eluted bead-free proteins were alkylated by incubating the samples with iodoacetamide (Sigma-Aldrich) and were subsequently subjected to digestion using trypsin (Promega, Madison, WI) at 4 μg/μL at 37°C. The following day, the reaction was stopped using 0.5% formic acid (Biosolve, Valkenswaard, the Netherlands) and peptides were subsequently evaporated at 30°C. Protein quantification was performed using the NanoOrange protein quantitation kit (Invitrogen, Waltham, MA).

### Liquid chromatography-mass spectrometry/mass spectrometry

A 1290 Infinity II ultra-high-performance liquid chromatography (LC) system (Agilent Technologies, Waldbronn, Germany) coupled with 6560 Ion mobility quadrupole time-of-flight ([IM-qTOF]; Agilent Technologies, Waldbronn, Germany) were used for all LC-mass spectrometry (MS) analyses. Separation was carried out on an Aeris Peptide XB-C18 column (150 × 2.1 mm ID; 1.7 μm) (Phenomenex, Torrance, CA) thermostated at 40°C. Mobile phase A and B consisted of H<sub>2</sub>O + 0.1% FA and ACN/H<sub>2</sub>O/FA (acetonitrile/water/formic acid; 90:10:0, v/v/v), respectively. Peptides were dissolved with an adequate volume of ACN/H<sub>2</sub>O/FA to reach 0.5 μg/μL per sample and 5 μg of peptides were injected on the column for each run. MS experiments were operated using positive electrospray ionization. For each sample, data were acquired using 2 acquisition modes, namely data-dependent acquisition (DDA) and data-independent acquisition (DIA), as previously described.<sup>18</sup>

### Data treatment and protein identification

Before protein identification, DIA MS/MS files were first reprocessed to recalibrate the mass axis using the reference masses. Then, LC and IM dimensions were smoothed using

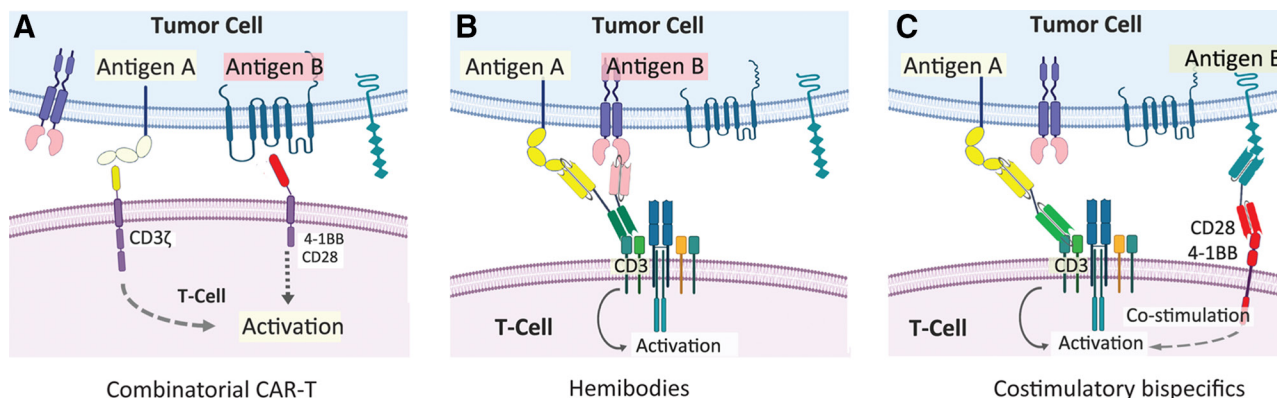


**Figure 1. Recently developed combinatorial strategies.** These strategies require that 2 antigens are present to activate immune effector cells. (A) They are based on the activation of costimulatory pathways in CAR-T cells; (B) the use of hemibodies with alignment of the CD3 binding heavy and light chain variable domains; and (C) the coadministration of bispecific antibodies that bind to a costimulatory receptor. CAR = chimeric antigen receptor.

PNNL PreProcessor software (Pacific Northwest National Laboratory, Richland, WA). Afterward, a 4D-IM feature extraction algorithm was applied on the datafile using peptides as isotope model, charge state no >7 and ion intensity above 50 in order to generate a list of ion features. Finally, extraction and alignment of MS/MS spectra with similar retention time ( $\pm 10$ s) and drift time ( $\pm 0.5$  ms) as the features were exported in a pickle (PKL) file.

DDA MS/MS files and PKL format files generated from DIA MS/MS were imported into Spectrum Mill Software (Agilent Technologies; Santa Clara, CA) for peptide sequencing. Carbamidomethylation of cysteines was selected as fixed modification and oxidation of methionines, deamidation of asparagines, and glutamines as well as carbamidomethylthio-propanoylation of lysines were selected as variable modifications. Trypsin was set as digestion enzyme and a maximum of 2 missed cleavages were allowed. Mass tolerance for precursor and product ions were set at 20 and 50 ppm, respectively. Peptides were considered as reliable hit by having a fragmentation score >5 and spectrum purity

index >50%. These peptides were exported for further statistical analysis.

**Subcellular localization and tissue distribution**

To define the subcellular localization and the protein expression in different organs, different databases (resumed in Table 1) were consulted. The Panther, COMPARTMENTS, and the Human Protein Atlas were used to confirm the cellular localization. For the Human Protein Atlas, the results with enhanced, approved, and supported reliabilities were retained for further analysis. To create a protein tissue distribution, expression values for different human tissues were obtained from the Human Protein Atlas, the Human Proteome Map (<http://www.humanproteomemap.org/download.php>, access date: May 29, 2019), the Proteomics Database (<https://www.proteomicsdb.org/proteomicsdb/#api>, access date: June 17, 2019), and a database composed of 29 healthy human tissues (PXD010154, access date: June 23, 2019).

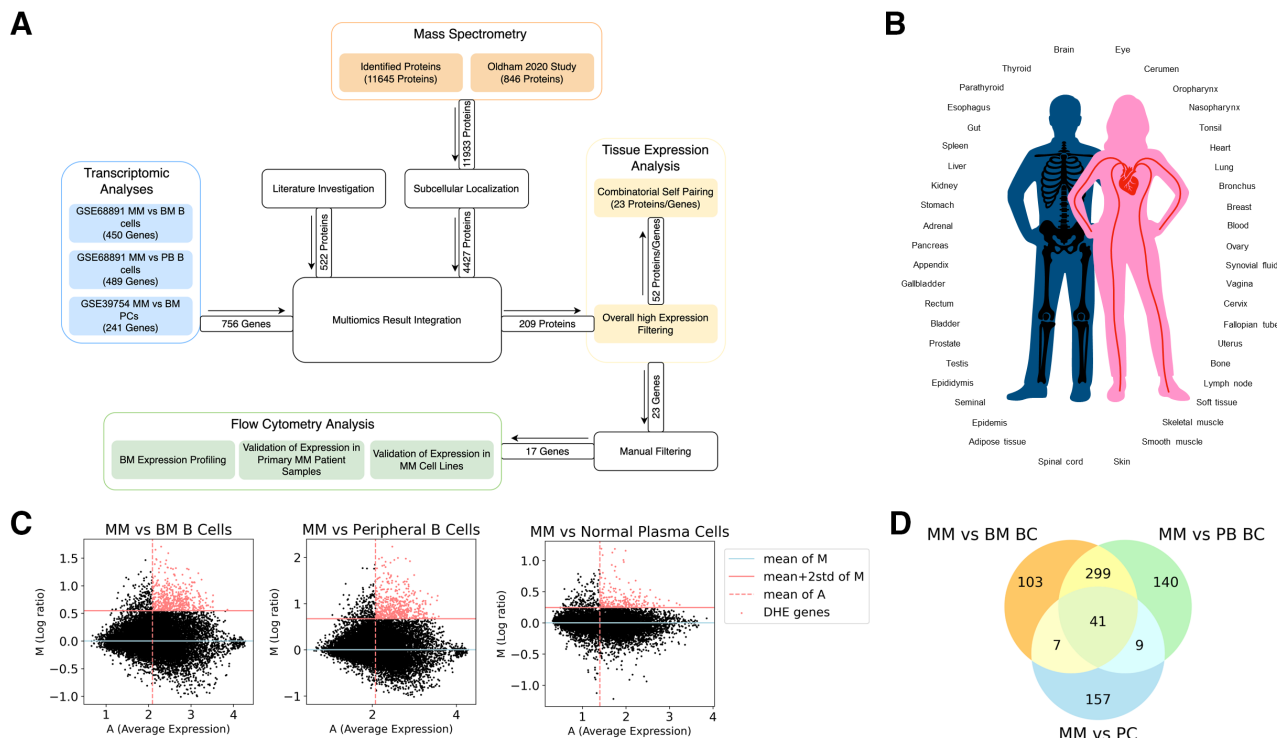


**Figure 2. Combinatorial target identification strategy.** (A) Analysis workflow. (B) The consensus tissue list. (C) MA plots (mean vs ratio) illustrating the identified DHE genes in different contrasts. DHE genes are genes with higher log ratios of mean + 2 SD and having higher expression than average expression among all patients. (D) Venn diagram representing the overlap of identified DHE genes in different contrasts. A = average expression; BM BC = bone marrow B cell; DHE = differentially highly expressed; M = log ratio; MM = multiple myeloma; PB BC = peripheral blood B cell; PC = plasma cell.

**Table 1**  
**The Different Databases That Were Consulted to Define the Exact Cellular Localization of Proteins**

Database Name	Website and Access Date	Retained Parameters	Additional Excluded Parameters
Panther database	<a href="https://www.pantherdb.org">https://www.pantherdb.org</a> September 24, 2019	Membrane, cell junction, extracellular membrane, and synapse	NA
COMPARTMENTS database	<a href="http://compartments.jensenlab.org">compartments.jensenlab.org</a> February 23, 2019	Plasma membrane, extracellular matrix, periphery, synapse, integrin complex, cell adhesion, cell surface, and extracellular region	Exclusion of cytoplasmic, cytoplasm, endosome, mitochondria, nuclear, nucleus, and exon were excluded
Human Protein Atlas	<a href="https://www.proteinatlas.org">https://www.proteinatlas.org</a> May 29, 2019	Cell junction, plasma membrane, focal adhesion sites, and peroxisomes	NA



### Expression binning and data aggregation

To visualize the tissue expression of these proteins, we merged information coming from proteomic studies performed on organ biopsies and further studied by immunohistochemistry or mass spectrometry. The protein expression values were categorized into 4 categories (not detected, low, medium, and high) based on the thresholds determined by mean-SD, mean, and mean + SD of Gaussian distribution fitted to log<sub>10</sub> values. All identifiers were converted into UniProt ID's. A consensus list of the different organs is shown in Figure 2B. For each dataset, tissues were binned into relative categories from the consensus list. Finally, all datasets were aggregated into a single dataset. All nomenclature conversions were applied by BioMart (<https://www.ensembl.org/biomart/martview/>). For nomenclature conversion and binning, in case of multiple annotations for the same entity, the higher value was always kept.

### Transcriptomics data retrieval and analysis

Experiment-normalized GSE68891 and GSE83503 (IFM) microarray datasets were downloaded.<sup>19,20</sup> GSE68891 dataset consists of MM cells (n = 126), peripheral blood B cells (n = 11), and BM B cells (n = 7).<sup>19</sup> Gene expression levels were compared between MM samples and 2 B-cell populations, respectively. On the contrary, in the IFM GSE83503 dataset, MM (n = 602) and plasma cell (n = 9) populations were compared.<sup>20</sup> For all comparisons (MM versus normal plasma cells, MM versus peripheral B cells, and MM versus BM B cells), MA (log ratio versus average) plots of MM versus control condition were generated. After fitting a Gaussian distribution with M values, the genes with higher values of M from mean + 2 SD, together with A values above the mean, were selected as differentially highly expressed (DHE) genes.

### Pairing strategy

Initially, the list of 11,645 candidate proteins, identified by mass spectrometry, was merged with the proteins identified in the Oldham 2020 study.<sup>21</sup> We analyzed articles, published between 1995 and 2021 and identified on Medline by using the keywords antigen, membrane, surface, and myeloma. This literature search retained 552 additional surface proteins. Our final list was filtered based on the subcellular localization. Furthermore, the proteins that were not coded by any of the DHE genes, those having a high expression in any nonimmune tissue, and those having overall high expression in all tissues were excluded. The remaining 52 proteins were paired with each other. The pairs that, in combination, had no expression in vital tissues and had at most low expression in nonvital tissues were selected as viable pairs (NA values were ignored).

### Identification of patient subgroups

The patients were categorized into transcriptomic subgroups using gene set variation analysis with signature genes identified by Zhan et al.<sup>22</sup> Copy number variation information of homologous recombination deficiency, t(4;14), t(11;14), t(14;16), CKS1B\_Gain (1q gain), CDKN2C\_Loss (1p loss), RB1\_Loss (Monosomy 13), BL\_TP53 (TP53 del), obtained from the Supplemental Digital Content provided by COMMPASS data, is used to classify patients into low-/high-risk categories based on the cytogenetic abnormalities.<sup>23</sup> Samples having 2 of the abnormalities t(4;14), 1q gain, 1p loss or 17p del, were categorized as double hit. Any sample having 3 of them is categorized as triple hit.

### Gene expression data scaling for visualization

To visualize the multiple datasets comparably, all expression values in each dataset were min-max scaled. In order to prevent any outlier effects on the high end of the distribution, the max value was replaced by the 99th percentile of the distribution.

### Staining by flow cytometry

Hemolysis (NH<sub>4</sub>Cl, 15 min) on the BM aspirates was first performed before carrying out membrane staining. These membrane staining were performed on different MM cell lines (LP-1, RPMI-8226, KMS-12-BM, U266, MOLP-2, OPM-2, NCI-H929, and MM1.S) and BM cells using the same protocol. Cells were incubated for 20 minutes at room temperature in the presence of predefined antibody concentrations. The cells were then fixed in 3% paraformaldehyde before being analyzed by flow cytometry. The anti-human antibodies used are listed in Suppl. Table S1. The anti-ET<sub>B</sub> monoclonal antibody (mAb) Rendomab B49 was produced after DNA-immunization of C57BL/6 mice and its affinities and binding epitopes determined.<sup>24,25</sup> For our flow cytometry studies, Rendomab49 (RB49) was directly conjugated to Alexa Fluor 488. Flow cytometry analyses were performed on a FACSCanto II flow cytometer (BD Biosciences, Franklin Lakes, NJ) and data were analyzed using BD FACSDiva Software V10 (BD Biosciences) or Kaluza V2.1 (Beckman Coulter, Brea, CA). BM samples from 13 newly diagnosed MM patients, 7 patients with relapsed/refractory disease, and 18 healthy persons were obtained and used for the validation of the antigen expression. Clinical data of the MM patients can be found in Suppl. Table S2.

## RESULTS

### Immunotherapeutic candidates detected by integrated analysis of proteomics and transcriptomics

By applying surface proteomics on 6 different cell lines and subsequent mass spectrometry, we identified 11,645 proteins. We added 846 proteins identified in the Oldham 2020 study.<sup>21</sup> Three data sources that describe the subcellular protein localization (Human Protein Atlas, Compartment, and PantherDB) were able to reduce this list to 4427 proteins that are known to be expressed on the cell membrane. A literature search identified 522 proteins that were added to this list.

An ideal target for immunotherapy should be (over) expressed on tumor cells and absent on normal tissue counterparts. We accessed the GSE83503 dataset that included microarray data of malignant plasma cells taken from 602 MM patients and normal plasma cells from 9 healthy volunteers. Contrasting expression profiles of MM cells with normal plasma cells resulted in 214 DHE genes in MM cells (Figure 2C, right panel). We further analyzed the GSE68891 dataset comparing transcriptomics of MM cells from 144 MM patients with nonmalignant B cells, isolated from the peripheral blood (n = 11) and BM (n = 7), yielding 450 (Figure 2C, left panel) and 489 (Figure 2C, middle panel) DHE genes, respectively. Combining the results from both datasets, we obtained 756 genes (Figure 2D) encoding 2818 proteins. Mapping these results on cell surface proteins identified in proteomics analysis further narrowed down this list to 209 surface proteins that are overexpressed in myeloma cells.

In order to assess the expression levels of identified proteins throughout the body, a consensus list of 42 organ entities was created that was further subdivided in vital, nonvital, and immune tissues. Based on their tissue distribution, we removed proteins with a high protein expression in any tissue, except for immune tissues. We retained 52 proteins that could be used for further combinatorial pairing. Protein pairs were selected if 1 of the partner proteins showed no detection in a vital tissue. Similar selection criteria were proposed for nonvital tissues with the exception that a low expression of both antigens was allowed in these tissues. To prevent exclusion of candidates due to missing information, NA values were ignored. After applying these criteria, we identified 23 proteins (Table 2) with 55 possible combinations (Figure 3A, right panel). The tissue distribution of these 23 proteins can be found in Figure 3B, top

panel. We further checked the tissue distribution of existing immunotherapeutic targets (Figure 3B, bottom panel) and obtained possible pairs between our candidates and existing targets (Figure 3A, left panel). From this list, we removed the secreted protein DKK1 and 8 other proteins with a suspected intracellular localization, including UBE2QL1, VDR, NR1D1, ZNF385A, TRB1, PPARGC1A, TAPBPL, and FRMD6.

**Table 2**  
List of the 23 Proteins Identified by the Algorithm

Gene Name	Uniprot	Protein Names
UBE2QL1	A1L167	E2Q-like ubiquitin-conjugating enzyme 1
PLXNC1	O60486	Plexin-C1 (CD232)
PRL3	O75365	Protein-tyrosine phosphatase of regenerating liver 3
DKK1	O94907	Dickkopf-related protein 1
IL6R	P08887	Interleukin-6 receptor subunit alpha
VDR	P11473	Vitamin D3 receptor
ICAM2	P13598	Intercellular adhesion molecule 2 (CD102)
EPOR	P19235	Erythropoietin receptor
NR1D1	P20393	Nuclear receptor subfamily 1 group D member 1
ETB	P24530	Endothelin receptor type B
CD27	P26842	CD27 antigen
IL5RA	Q01344	IL-5R subunit alpha (CD125)
BCMA	Q02223	Tumor necrosis factor receptor superfamily member 17
FRMD6	Q96NE9	FERM domain-containing protein 6
ZNF385A	Q96PM9	Zinc finger protein 385A
TRB1	Q96RU8	Tribbles homolog 1
TAPBPL	Q9BX59	Tapasin-related protein
SLCO5A1	Q9H2Y9	Solute carrier organic anion transporter family member 5A1
SPAG4	Q9NPE6	Sperm-associated antigen 4 protein
PPARGC1A	Q9UBK2	PPAR-gamma coactivator 1-alpha
DEXRAS1	Q9Y272	Dexamethasone-induced Ras-related protein 1
CEACAM8	P31997	Carcinoembryonic antigen-related cell adhesion molecule 8
MC4R	P32245	Melanocortin receptor 4

Identification of 6 novel combinatorial targets

With flow cytometry, we checked the surface expression of the 14 remaining proteins and of 3 proteins with favorable tissue distribution already used in immunotherapeutic strategies (NY-ESO-1, CD70, and FCRL5) on 8 MM cell lines. Nevertheless, FCRL5 was not analyzed at this stage as it is known to be expressed by only 1 MM cell line namely MOLP-2 cell line. Table 3 summarizes the presence and expression levels of these proteins on the cell lines. The expression of IL5RA, SPAG4, NY-ESO-1, and EPOR could not be confirmed. ET<sub>B</sub> was expressed by all cell lines, PLXNC1 by 7, BCMA, MC4R, and SLCO5A1 by 6, PRL3, IL6R, and ICAM2 by 5, DEXRAS1 by 4, CD70 by 3, and CD27 and CEACAM8 by only one of the cell lines. Targets that were not detected or that were only detected in 1 cell line were eliminated. Thus, based on these expression profiles, the list of potential candidates was narrowed down to 10 remaining proteins for further studies on primary patient samples.

Indeed, the expression of individual proteins was subsequently checked on BM samples of 20 MM patients (Table 4). FCRL5 was included in the analysis at this step. All the targets could be detected but with variable expression frequencies. FCRL5, BCMA, and ICAM2 were expressed by all patients, IL6R by 85%, ET<sub>B</sub> by 75%, SLCO5A1 by 65%, and PRL3 by 50%, while MC4R, DEXRAS1, CD70, and PLXNC1 were only expressed by 14%–36% of patients.

To avoid toxicity on hematopoietic stem cells or immune effector cells (T and natural killer [NK] cells), we evaluated the expression of these 11 proteins on samples of normal plasma cells, T and NK cells, as well as CD34<sup>+</sup> HSC from 18 healthy donors (Figure 4A and Suppl. Tables S3-S5).

An additional selection criterion for pairing was based on the protein expression on these normal BM populations. Indeed, potential pairs that showed a potential expression on normal BM cells were filtered out. Moreover, only the pairs with viable combinatorial tissue expression were retained. The remaining pairs were further investigated for their combined expression frequency on MM cells (Figure 4B). The pairs with a combined expression frequency

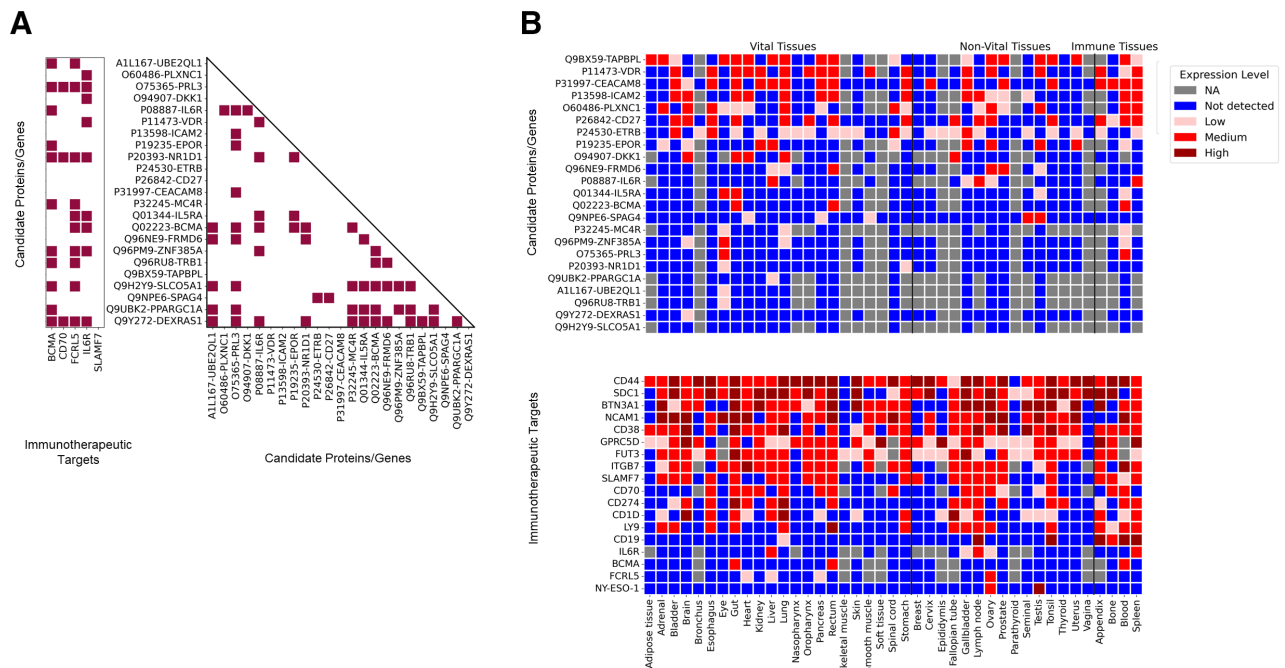


**Figure 3. Tissue expression and pairing of candidate and existing immunotherapeutic targets.** (A) Viable pairs between candidate proteins/genes and existing immunotherapeutic targets (left) as well as self-combinations (right). Viable pairs are selected based on having no expression in vital tissues and at most low expression in nonvital tissues as pairs. (B) Tissue expression of candidate proteins/genes (top) and existing immunotherapeutic targets (bottom).

**Table 3**  
Frequencies of Expression of 16 Target Antigens on 8 MM Cell Lines

	LP-1	RPMI-8226	MOLP-2	U266	OPM-2	KMS-12-BM	NCI-H929	MM1.S	Freq. of Exp. (%)	Expression Levels (%)		
										+++	++	+
PLXNC1	+	++	++	+	-	++	++	++	<b>87.5</b>	0	71.4	28.6
PRL3	++	-	-	++	-	+	++	+++	<b>62.5</b>	20	60	20
IL6R	+	++	+++	++	-	++	-	-	<b>62.5</b>	20	60	20
ICAM2	+++	+++	+++	+++	-	+++	-	-	<b>62.5</b>	100	0	0
EPOR	-	-	-	-	-	-	-	-	<b>0</b>	0	0	0
ETB	+	++	++	+++	+	+	+	+	<b>100</b>	12.5	25	62.5
CEACAM8	-	-	-	-	-	-	-	+	<b>12.5</b>	0	0	100
MC4R	+	-	+	++	-	+	+	+	<b>75</b>	0	16.7	83.3
IL5RA	-	-	-	-	-	-	-	-	<b>0</b>	0	0	0
BCMA	++	+	+	-	-	+++	+++	++	<b>75</b>	33.3	33.3	33.3
CD27	-	-	-	-	-	+	-	-	<b>12.5</b>	0	0	100
SLC05A1	+	+	+	+++	+	++	-	-	<b>75</b>	16.7	33.3	66.7
SPAG4	-	-	-	-	-	-	-	-	<b>0</b>	0	0	0
DEXRAS1	+	-	-	+	-	-	+	+	<b>50</b>	0	0	100
NY-ESO-1	-	-	-	-	-	-	-	-	<b>0</b>	0	0	0
CD70	+++	-	-	+++	-	++	-	-	<b>37.5</b>	66.7	33.3	0

The values in bold correspond to the expression frequencies (%) of each target in the tested population.  
MM = multiple myeloma; - = negative cells; + = low positive cells; ++ = intermediate positive cells; +++ = high positive cells.

**Table 4**  
Frequencies of Expression of 11 Target Antigens on Myeloma Plasma Cells From the Bone Marrow of MM Patients

	ETB	MC4R	ICAM2	DEXRAS1	CD70	FCRL5	SLC05A1	IL6R	BCMA	PLXNC1	PRL3	
Patient 1	ND	ND	ND	ND	ND	+	+	+	+	ND	ND	
Patient 2	+	+	ND	ND	-	+	+	+	+	ND	+	
Patient 3	ND	ND	ND	ND	-	+	+	+	+	ND	+/-	
Patient 4	+	-	ND	ND	-	+/-	+/-	-	+	ND	+/-	
Patient 5	ND	ND	ND	ND	-	+	+	+	+	ND	+/-	
Patient 6	+/-	-	ND	ND	-	+	-	+/-	+/-	ND	+/-	
Patient 7	+/-	-	ND	ND	-	+	+	+	+	ND	-	
Patient 8	ND	ND	ND	ND	-	+	+/-	+	+	ND	-	
Patient 9	+/-	+/-	ND	ND	-	+	+	+	+	ND	+	
Patient 10	+	+/-	ND	ND	-	+	+	+	+	ND	-	
Patient 11	+/-	+/-	ND	ND	-	+	-	+	+/-	ND	-	
Patient 12	ND	ND	ND	ND	-	+	+	+	+	ND	+/-	
Patient 13	ND	ND	ND	ND	-	+	+/-	+	+	ND	ND	
Patient 14	+	-	+	-	+	+	+/-	-	+	+	+	
Patient 15	-	-	+	+	+/-	+	+/-	-	+	-	-	
Patient 16	+/-	-	+	-	+	+	-	+	+	-	-	
Patient 17	-	-	+	-	+/-	+	-	+/-	+	-	+/-	
Patient 18	-	+	+	ND	-	+	-	+	+	-	-	
Patient 19	ND	-	+	+/-	-	+	-	+	+	-	-	
Patient 20	ND	-	+	-	-	+	-	+	+	-	-	
Freq. of exp. (%)		<b>75</b>	<b>35.7</b>	<b>100</b>	<b>33.3</b>	<b>21.1</b>	<b>100</b>	<b>65</b>	<b>85</b>	<b>100</b>	<b>14.3</b>	<b>50</b>
Freq. of exp. among + cells (%)	+	44.4	40	100	50	50	95	61.5	88.2	90	100	33.3
	+/-	55.6	60	0	50	50	5	38.5	11.8	10	0	66.7

The last 2 lines of the table show the distribution of the expression frequencies between the positive cells and the partial positive cells among the total positive cells.  
Freq. of exp. = frequency of expression; MM = multiple myeloma; ND = not determined; - = negative cells; +/- = partial positive cells; + = positive cells.

of >40% (2 of which were >70%) were selected as top findings (Figure 4C).

Concerning off target toxicity, we prioritized no expression in any vital organs and tolerated at most low expression in nonvital organs. However, a more stringent analysis where the target expression is not tolerated in any tissue, except for immune tissues, is valuable. Increasing the stringency of the selection criteria removed 7 possible pairs identified at the initial step of our analysis (Suppl. Figure S1) but did not affect the final results obtained validating the antigen expression on primary myeloma cells by flow cytometry.

**Transcriptional profiles of target antigens in transcriptional and cytogenic patient subgroups**

MM remains a heterogeneous disease with biological differences in tumor development and associated clinical outcomes. From a molecular point of view, the transcriptional profiles of patients can be categorized based on the University of Arkansas for Medical Science (UAMS) classification proposed by Zhan et al.<sup>22</sup> Using the GSE83503 dataset, we categorized patients into UAMS categories and compared gene expression in plasma cells from healthy donors and myeloma patients (Figure 5A). We observed a heterogeneous expression of our identified proteins

Downloaded from https://journals.lww.com/jemasphere by BMDI/SePh/Kav1/Zeoun11QIN/4a+k/LHEZgphs/Ho4/XMh/CV WOX1AWNhy/Qp/IIQH/D3/3D000dRy/7TVS/FI4C/3VCA/OAVp/Da8K2+YagH515KE= on 03/01/2024

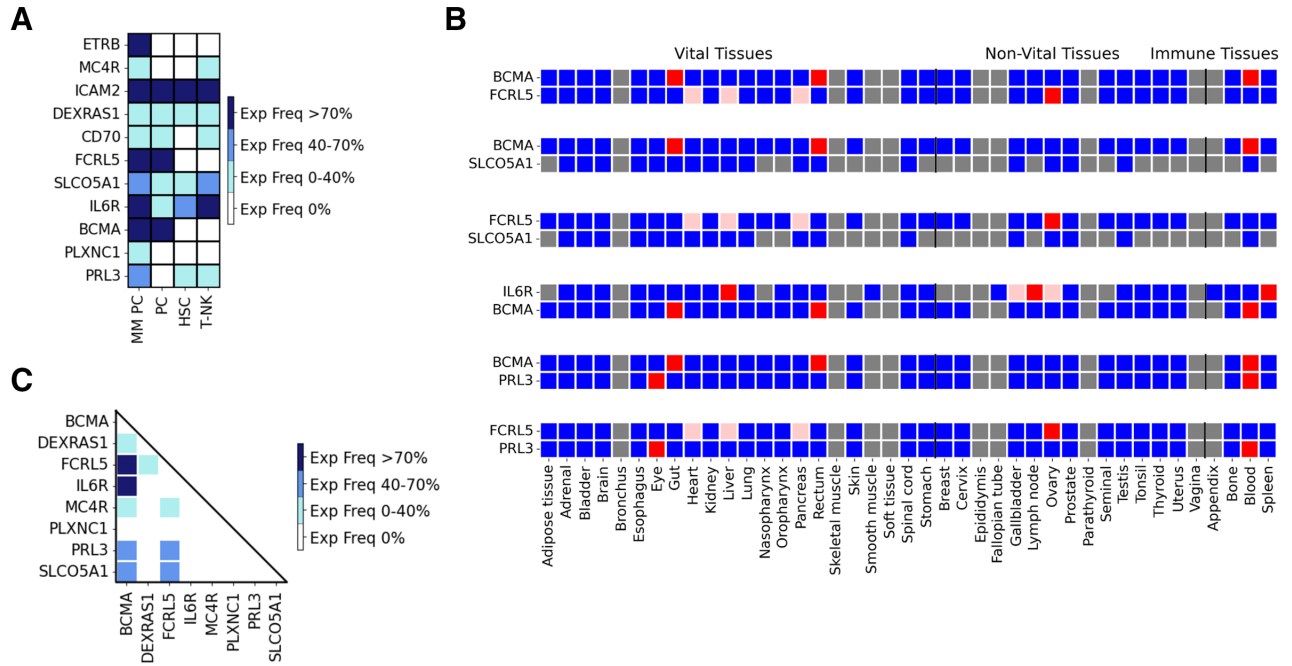


**Figure 4. Selection of ideal combinatorial pairs.** (A) The frequencies of expression of candidate genes on MM PC from the bone marrow of MM patients and on normal PC, normal CD34+ HSC, normal T and NK cells (T-NK) from the BM of healthy donors. (B) Tissue expression distributions of the genes in the top combinatorial target pairs. (C) The combined expression levels for each possible pair in MM cells. BM = bone marrow; HSC = hematopoietic stem cells; MM = multiple myeloma; PC = plasma cells.

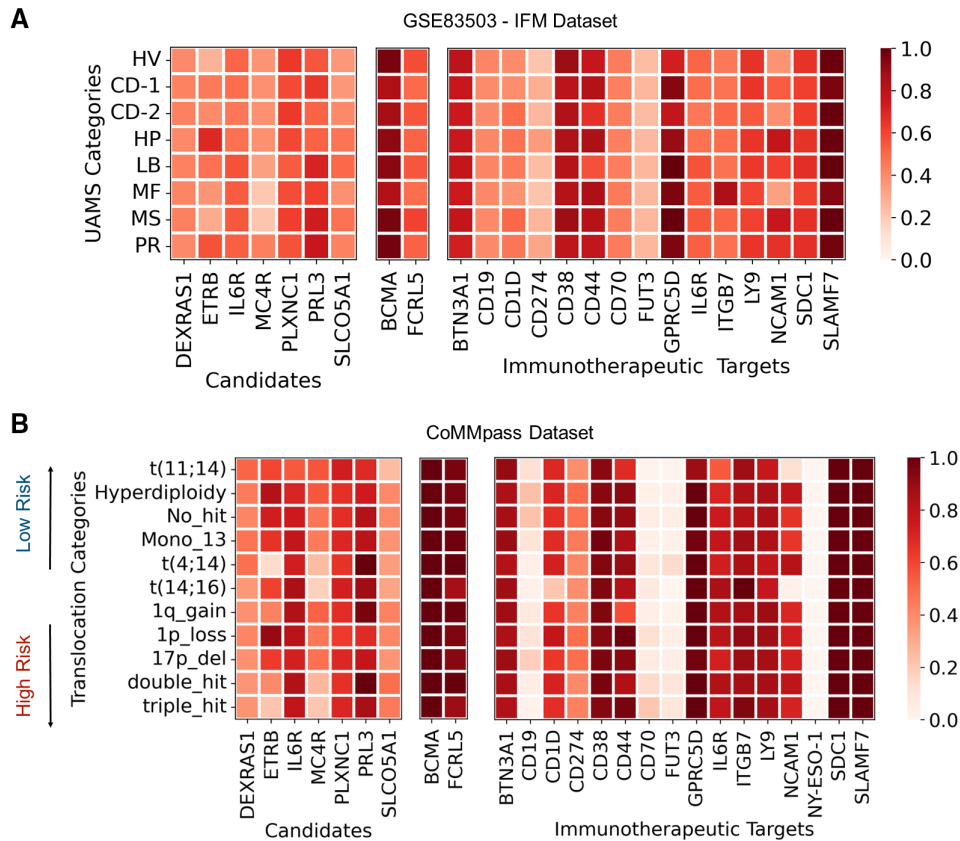


**Figure 5. Median expression (scaled) profiles of genes among transcriptional and cytogenetic patient categories.** (A) Median expression profiles of candidate and immunotherapeutic target genes over UAMS categories in the IFM dataset (GSE83503). (B) Median expression profiles of candidate and immunotherapeutic target genes over cytogenetic categories in the CoMMpass dataset. In both datasets, the data is min-max scaled using 99th percentile as the maximum value.



*ETB*, *MC4R*, *PRL3*, and the current targets for immunotherapy *CD44*, *ITGB7*, *NCAM1*. This heterogeneity was confirmed in the COMMPASS dataset that we used as a validation cohort of our results (Suppl. Figure S2).

A more clinically relevant categorization can be made based on the cytogenetic abnormalities that are only available in the COMMPASS dataset and have recently been annotated.<sup>23</sup> The identified cytogenetic abnormalities can be categorized into low-risk, standard-risk, and high-risk groups. Notably, the heterogeneity observed in the molecular classification was also observed in this patient stratification (Figure 5B). In both datasets, immunotherapeutic targets *BCMA*, *FCRL5*, *CD38*, *GPRC5D*, *SDC1* (*CD138*), and *SLAMF7* stood out with consistent high-expression levels in all patient subgroups. From our candidates, *IL6R* and *PRL3* can also be added to this list.

**ET<sub>B</sub> as a single target**

Our study revealed ET<sub>B</sub> as a potential target for MM. This protein was expressed by MM cell lines and primary myeloma cells (results from one of these patients is illustrated in Figure 6C). It also presented a global low expression profile throughout the body (Figure 3B). Inside the BM, ET<sub>B</sub> is only expressed by MM plasma cells. These results were confirmed by single-cell RNA studies on CD38<sup>+</sup> purified myeloma cells and other BM cells from 13 MM subjects (Figure 6A).<sup>26</sup> Moreover, the expression of ET<sub>B</sub> has prognostic significance. In the COMMPASS data set, patients with a high ET<sub>B</sub> mRNA level had better overall survival compared with patients with low ET<sub>B</sub> mRNA levels (Figure 6D). This survival benefit can be explained by a lower mRNA expression in patients with high-risk cytogenetics such as t(4;14), double hit and triple hit abnormalities (Figure 6B). When looking at the level of mRNA expression in the different molecular subgroups, the MS-subgroup (overexpression of

*FGFR3* and *MMSET* genes induced by t[4;14]) displayed lower expression compared with other subgroups (Suppl. Figure S3). ET<sub>B</sub> is a G-protein-coupled receptor that changes its confirmation upon activation with new epitopes becoming exposed.<sup>28</sup> Rendomab B49 is a murine IgG1kappa mAb that recognizes such an epitope near the N-terminal of the receptor.<sup>25</sup> We obtained the RB49 antibody conjugated to Alexa Fluor 488 and compared its binding to primary myeloma cells with the binding of a control IgG1k antibody. In 8 of the 10 (80%) tested primary MM samples, we could confirm the binding of RB49 to primary malignant plasma cells (results from one of these patients is illustrated in Figure 6E). Patient characteristics and obtained flow cytometry results can be found in Suppl. Table S6.

**DISCUSSION**

MM is a highly heterogeneous and dynamic disease in which immune dysfunction plays an important role in disease pathogenesis, progression, and drug resistance.<sup>29</sup> Although patients may have long responses to treatment, most of them will eventually develop treatment-resistant disease. Recently, new personalized treatment approaches, such as immunotherapy, that offer the advantage of specifically targeting tumor cells have been developed.

Herein, we present an approach that enables the discovery of new immunotherapeutic targets in MM. We have assembled a comprehensive MM surfaceome dataset, combining previously published protein repositories, transcriptomic data that compared RNA of myeloma cells with normal plasma cells and B cells, and our own cell surface proteomics performed on 6 MM cell lines. We added data on tissue distribution to take into account the systemic expression of potential targets and to avoid toxicity in healthy organs.

The expression of 11 candidate targets was verified by flow cytometry on BM samples from 20 MM patients and 18 healthy

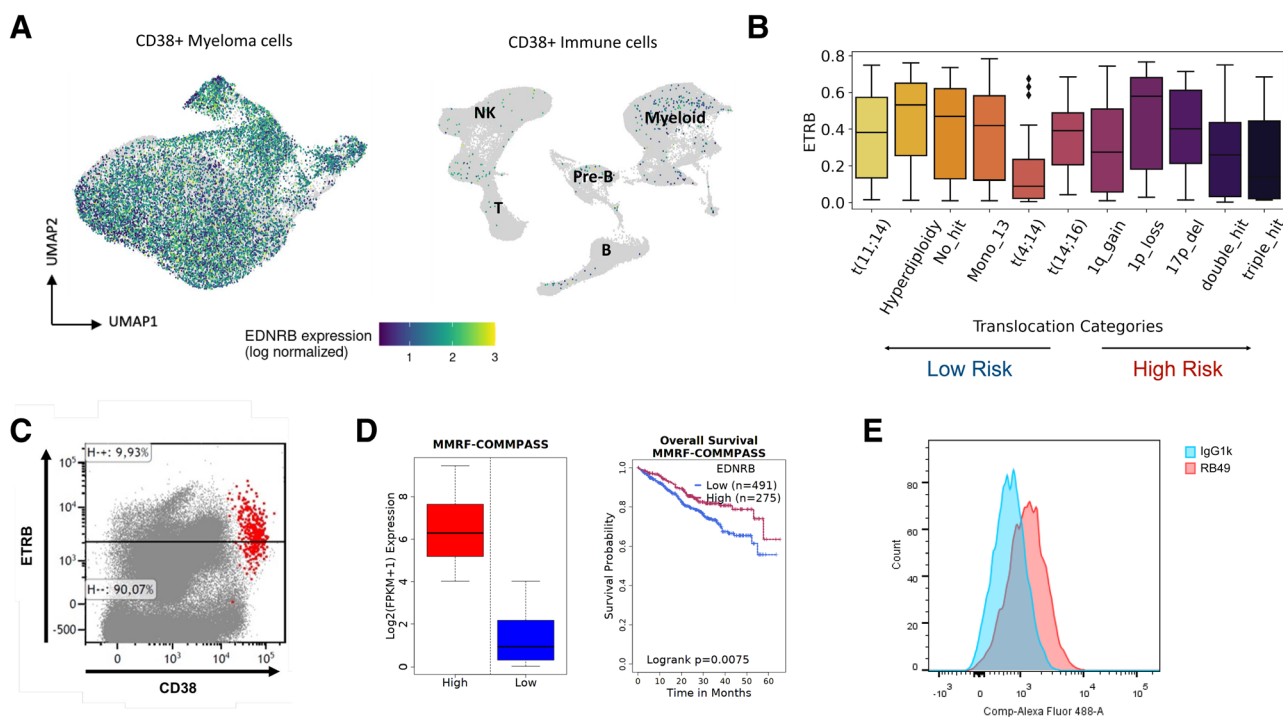


**Figure 6. The expression profiles of ET<sub>B</sub> gene at proteomic and transcriptional level as well as in different patient subgroups.** (A) Transcriptomic expression of ET<sub>B</sub> (EDNRB) at single-cell level in bone marrow shown among myeloma plasma cells (left) obtained from 13 MM subjects, and CD38<sup>+</sup> immune cells (right) obtained from 13 MM and 5 healthy subjects.<sup>26</sup> (B) Expression profile among different cytogenetic categories in COMMPASS dataset. (C) Flow cytometry analysis conducted on the bone marrow sample from MM patient 10, as a sample. The population in red represents CD38<sup>+</sup> MM plasma cells. (D) Results of the survival analysis conducted by SurvivalGenie.<sup>27</sup> Patients in the COMMPASS dataset are divided into low- and high-expression categories using the cutp option (left) and survival analysis is performed (right). (E) Histogram illustrating the flow cytometry results with the control IgG1k (in blue) and RB49 (in red), confirming the expression of ET<sub>B</sub>. ETB = endothelin receptor B; MM = multiple myeloma.

donors. Seven of them ( $ET_B$ , ICAM2, FCRL5, SLC05A1, IL6R, and BCMA) were detected in >50% of MM patients' BM. Among these targets, ICAM2, SLC05A1, and IL6R were found on normal T-NK cells and/or on CD34<sup>+</sup> HSC and could potentially lead to fratricide of effector cells or in the elimination of hematopoietic stem cells. The remaining 3 targets, BCMA, FCRL5, and  $ET_B$ , have favorable expression profiles. BCMA and FCRL5 have already been tested in the context of MM in immunotherapeutic strategies such as CAR-T cells, antibody-drug conjugates, BsAbs, etc. In contrast,  $ET_B$ , a G-protein coupled receptor, has been scarcely studied in the context of MM.

The endothelin axis is involved in the development of an increasing number of tumors, by affecting cell proliferation, migration, invasion, epithelial-mesenchymal transition, osteogenesis, and angiogenesis.<sup>30</sup> Vaiou et al<sup>31</sup> showed that endothelin-1 (ET-1) supports MM cell viability through both autocrine and paracrine activation, because both myeloma cells and endothelial cells produce ET-1. ET-1 binds to 2 receptors:  $ET_A$  and  $ET_B$ , and its downstream effects are mediated by the MAP kinase pathway and ubiquitin proteasome system. Addition of selective agonists of ETRA or  $ET_B$  or with the dual receptor antagonists bosentan or macitentan resulted in a significantly decreased viability of MM cell lines.<sup>32,33</sup> More recently, the same group treated MM xenograft models with macitentan, which resulted in reduced tumor load and myeloma-induced angiogenesis; both explained by an inhibitory effect on HIF-1 alpha and secretion of angiogenic cytokines.<sup>34</sup> Although ET-1 supports MM cell survival and antagonists of  $ET_A$  and  $ET_B$  are able to reduce MM cell growth, CRISPR screens could not confirm a dependency of MM cell lines to  $ET_B$  for their survival (Suppl. Figure S3).

As shown in Figure 6,  $ET_B$  is well expressed by MM cells, has a favorable tissue distribution, and shows high expression among the majority of patient subgroups. Upon activation and binding of endothelin, this receptor changes its conformation.<sup>28</sup> Hosen et al<sup>35</sup> demonstrated that the active conformer of a protein can serve as a specific therapeutic target, as it is the case with integrin  $\beta 7$ . Indeed, these authors identified a mAb specifically targeting the N-terminal region of the  $\beta 7$  chain, which is inaccessible when the integrin is quiescent but exposed in the active conformation. Herbert et al<sup>25</sup> demonstrated that this is also the case with  $ET_B$ . They produced different mAbs targeting this receptor, including RB49, which binds to an epitope located in the N-terminal domain of  $ET_B$ . In this work, we show that RB49 binds to MM cells and we believe that its sequences can be integrated into different immunotherapy strategies such as CAR-T cells, BsAbs, etc, for the treatment of MM.

However, our study has some limitations. Indeed, the selection of potential targets is partially based on the flow cytometry results, which can be impacted by several parameters. A major limitation is the need for specific antibodies, preferentially coupled to a fluorochrome. By limiting ourselves to the antibodies available on the market, we had to use monoclonal antibodies for certain targets and polyclonal antibodies for others. In addition, each fluorochrome can potentially influence other fluorochromes and the required compensation may result in a loss of sensitivity and resolution. Thus, weakly expressed antigens may not be detected by flow cytometry analysis. Finally, the brightness of the fluorochromes used also has an impact on the quality of the results.

The restrictive criteria that we proposed to further narrow down our selection is a second limitation of our study. Certain proteins already known and studied at present, which did not meet the selection criteria, were eliminated. For example, CD38 and GPRC5D did not have a favorable tissue expression profile were removed from the list while their use has already been shown to be beneficial for the treatment of MM.

Finally, for practical reasons, we used MM cell lines in order to make a preselection of proteins before moving on to primary cell samples. However, cell lines, lacking certain adhesion molecules, growth factor, or chemokine receptors, are not completely

representative of tumor cells of the patients. Indeed, because FCRL5 is only expressed by a single MM cell line, we did not include it in the validation studies on cell lines, although it is expressed by all patients. Thus, other targets with a limited expression on the different cell lines are potentially missed at the first stages.

However, our algorithm can become a powerful tool for antigen identification, but researchers should be aware that the selection criteria for retaining potential antigens may eliminate potentially interesting proteins. These criteria were that stringent to retain the most suitable targets (based on the membrane localization and tissue distribution) and to avoid retention of false-positive proteins. The advantage of such an algorithm is that it can be modified according to the tumor type and application: targets of antibody-drug conjugates should internalize after ligation of antibodies and immunotherapeutic targets should have an absent off-tumor expression. Due to the low homogeneity of target expression and the possibility of immune recognition escape and relapse, combinatorial targeting approaches are now being investigated. Our algorithm has highlighted 6 possible pairs that would be interesting to analyze more in depth in strategies such as CAR-T/NK or BsAb.

MM is an extremely heterogenous disease, with major differences in disease presentation and complications, response to treatment, and overall survival. Both molecular and cytogenetic differences drive this heterogeneity. Our results indicate that antigen expression also vary between patients and patient groups: this was particularly true for  $ET_B$ , NCAM1, IL6R, ITB7, and CD44. On the contrary, integration of mRNA expression results from different cytogenetic subgroups allows identification of more specific antigens or antigen pairs. By integrating the COMMPASS dataset and annotating the different molecular or cytogenetic subgroups, we were able to identify combinatorial pairs that could potentially be used for patients in those subgroups. This COMPASS dataset contains whole genome, whole exome, and RNA sequencing results. Although there is a good correlation between mRNA and protein levels in general in cancer,<sup>36</sup> we find it worth to look at protein levels in future studies on immunotherapeutic targets in specific MM patient subgroups.

The identification of new potential targets is a growing field in MM. Oldham et al<sup>21</sup> and Ferguson et al<sup>37</sup> focused on membrane glycoproteins, while Di Meo et al,<sup>38</sup> Anderson et al,<sup>39</sup> and ourselves analyzed the entire set of surface proteins. The obtained datasets were either used alone or combined with transcriptomic datasets. The initial sample manipulation and sensitivity of mass spectrometry analysis may also differ from assay to assay. Thus, each study will not provide the same list of candidates, and candidates must be confirmed by other analyses. For example, Di Meo et al<sup>38</sup> demonstrated 3 proteins (CCR1, LRRC8D, and SEMA4A) whose inactivation individually reduces the in vitro growth of MM cells by ~60%, 50%, and 50%, respectively. Anderson et al<sup>39</sup> confirmed the unique expression of SEMA4A and found that downregulating its expression using shRNA decreased myeloma cell proliferation, increased apoptosis, and delayed tumor growth. Moreover, an antibody-drug conjugate binding to SEMA4A showed enhanced cytotoxic effects in vitro and in vivo. In our study, the SEMA4A protein was part of the initial list, but was eliminated at the differential expression stage. Our thresholds are probably more stringent than those used in the 2 previous studies.

## CONCLUSIONS

By integrating proteomics, transcriptomics, and datasets on tissue distribution, we identified several candidate antigens that can be used for either single-antigen targeting approaches or for combinatorial targeting.  $ET_B$  seems a promising antigen because of its restricted expression on malignant myeloma cells and conformational change in protein structure upon activation. In addition,

combinations of either existing or previously unknown antigens could be proposed. These combinations can be integrated into more selective therapies by avoiding on-target, off-tumor toxicity.

#### ACKNOWLEDGMENTS

The authors thank Stéphane Minvielle for providing the extended GSE83503 dataset and the laboratory of Hematology (CHU de Liège) and the GIGA Cell Imaging and Flow Cytometry platform (ULiège) for their excellent technical assistance.

#### AUTHOR CONTRIBUTIONS

ML, MCK, MF, and JC designed the studies. ML, MCK, MJ, ED, GC, and JF performed experiments and analyzed the data. DB and AH provided pivotal material for the study. ML, MCK, and JC wrote the article. MG, AH, DB, GC, and MF provided additional input for the article. All authors read and approved the article.

#### DISCLOSURES

DB and AH are scientific cofounders and hold equity in Skymab Biotherapeutics. All the other authors have no conflicts of interest to disclose.

#### DATA AND METHODS AVAILABILITY

The lists of the 209 proteins overexpressed in MM cells (DiffExpMembraneProteins.txt) and of the 52 proteins (DiffExpMembraneProteinsTissueFiltered.txt) filtered based on their tissue expression were generated in this study. These data are available upon request.

#### SOURCES OF FUNDING

The laboratory of Hematology was supported by the Foundation Against Cancer, ERA-NET Transcan (SMARTCAR project), the Fonds National de la Recherche Scientifique (F.N.R.S., Belgium), The Foundation Léon Frédéricq, the CHU de Liège and the Fonds spéciaux de la Recherche (University of Liège).

#### REFERENCES

- Brink M, Groen K, Sonneveld P, et al. Decrease in early mortality for newly diagnosed multiple myeloma patients in the Netherlands: a population-based study. *Blood Cancer J*. 2021;11:178.
- Lonial S, Weiss BM, Usmani SZ, et al. Daratumumab monotherapy in patients with treatment-refractory multiple myeloma (SIRIUS): an open-label, randomised, phase 2 trial. *Lancet*. 2016;387:1551–1560.
- Dimopoulos MA, Oriol A, Nahi H, et al. Daratumumab, lenalidomide, and dexamethasone for multiple myeloma. *N Engl J Med*. 2016;375:1319–1331.
- Palumbo A, Chanan-Khan A, Weisel K, et al. Daratumumab, bortezomib, and dexamethasone for multiple myeloma. *N Engl J Med*. 2016;375:754–766.
- Facon T, Kumar S, Plesner T, et al. Daratumumab plus lenalidomide and dexamethasone for untreated myeloma. *N Engl J Med*. 2019;380:2104–2115.
- Voorhees PM, Kaufman JL, Laubach J, et al. Daratumumab, lenalidomide, bortezomib, and dexamethasone for transplant-eligible newly diagnosed multiple myeloma: the GRIFFIN trial. *Blood*. 2020;136:936–945.
- Batlevi CL, Matsuki E, Brentjens RJ, et al. Novel immunotherapies in lymphoid malignancies. *Nat Rev Clin Oncol*. 2016;13:25–40.
- Lejeune M, Köse MC, Duray E, et al. Bispecific, T-cell-recruiting antibodies in B-cell malignancies. *Front Immunol*. 2020;11:762.
- Cho SF, Xing L, Anderson KC, et al. Promising antigens for the new frontier of targeted immunotherapy in multiple myeloma. *Cancers (Basel)*. 2021;13:6136.
- Swamydas M, Murphy EV, Ignatz-Hoover JJ, et al. Deciphering mechanisms of immune escape to inform immunotherapeutic strategies in multiple myeloma. *J Hematol Oncol*. 2022;15:17.
- Samur MK, Fulciniti M, Aktas Samur A, et al. Biallelic loss of BCMA as a resistance mechanism to CAR T cell therapy in a patient with multiple myeloma. *Nat Commun*. 2021;12:868.
- Da Vià MC, Dietrich O, Truger M, et al. Homozygous BCMA gene deletion in response to anti-BCMA CAR T cells in a patient with multiple myeloma. *Nat Med*. 2021;27:616–619.

- Burgos L, Puig N, Cedena MT, et al. Measurable residual disease in multiple myeloma: ready for clinical practice? *J Hematol Oncol*. 2020;13:82.
- Kloss CC, Condomines M, Cartellieri M, et al. Combinatorial antigen recognition with balanced signaling promotes selective tumor eradication by engineered T cells. *Nat Biotechnol*. 2013;31:71–75.
- Perna F, Berman SH, Soni RK, et al. Integrating proteomics and transcriptomics for systematic combinatorial chimeric antigen receptor therapy of AML. *Cancer Cell*. 2017;32:506–519.e5.
- Banaszek A, Bumm TGP, Nowotny B, et al. On-target restoration of a split T cell-engaging antibody for precision immunotherapy. *Nat Commun*. 2019;10:5387.
- Skokos D, Waite JC, Haber L, et al. A class of costimulatory CD28-bispecific antibodies that enhance the antitumor activity of CD3-bispecific antibodies. *Sci Transl Med*. 2020;12:eaaw7888.
- Nys G, Nix C, Cobraville G, et al. Enhancing protein discoverability by data independent acquisition assisted by ion mobility mass spectrometry. *Talanta*. 2020;213:120812.
- Martello M, Poletti A, Borsi E, et al. Clonal and subclonal TP53 molecular impairment is associated with prognosis and progression in multiple myeloma. *Blood Cancer J*. 2022;12:15.
- Mianny B, Minvielle S, Roux O, et al. Logic programming reveals alteration of key transcription factors in multiple myeloma. *Sci Rep*. 2017;7:9257.
- Oldham RAA, Faber ML, Keppel TR, et al. Discovery and validation of surface N-glycoproteins in MM cell lines and patient samples uncovers immunotherapy targets. *J ImmunoTher Cancer*. 2020;8:e000915.
- Zhan F, Huang Y, Colla S, et al. The molecular classification of multiple myeloma. *Blood*. 2006;108:2020–2028.
- Walker BA, Mavrommatis K, Wardell CP, et al. Identification of novel mutational drivers reveals oncogene dependencies in multiple myeloma. *Blood*. 2018;132:587–597.
- Allard B, Wijkhuisen A, Borrull A, et al. Generation and characterization of rendomab-B1, a monoclonal antibody displaying potent and specific antagonism of the human endothelin B receptor. *MABS*. 2013;5:56–69.
- Herbet A, Costa N, Leventoux N, et al. Antibodies targeting human endothelin-1 receptors reveal different conformational states in cancer cells. *Physiol Res*. 2018;67(Suppl 1):S257–S264.
- de Jong MME, Kellermayer Z, Papazian N, et al. The multiple myeloma microenvironment is defined by an inflammatory stromal cell landscape. *Nat Immunol*. 2021;22:769–780.
- Dwivedi B, Mumme H, Satpathy S, et al. Survival Genie, a web platform for survival analysis across pediatric and adult cancers. *Sci Rep*. 2022;12:3069.
- Shihoya W, Nishizawa T, Okuta A, et al. Activation mechanism of endothelin ET(B) receptor by endothelin-1. *Nature*. 2016;537:363–368.
- Visram A, Kourelis TV. Aging-associated immune system changes in multiple myeloma: The dark side of the moon. *Cancer Treat Res Commun*. 2021;29:100494.
- Rosano L, Spinella F, Bagnato A. Endothelin 1 in cancer: biological implications and therapeutic opportunities. *Nat Rev Cancer*. 2013;13:637–651.
- Vaiou M, Pangou E, Liakos P, et al. Endothelin-1 (ET-1) induces resistance to bortezomib in human multiple myeloma cells via a pathway involving the ETB receptor and upregulation of proteasomal activity. *J Cancer Res Clin Oncol*. 2016;142:2141–2158.
- Russignan A, Spina C, Tamassia N, et al. Endothelin-1 receptor blockade as new possible therapeutic approach in multiple myeloma. *Br J Haematol*. 2017;178:781–793.
- Russignan A, Spina C, Tamassia N, et al. In reply to Schäfer et al: new evidence on the role of endothelin-1 axis as a potential therapeutic target in multiple myeloma. *Br J Haematol Eng*. 2019;184:1052–1055.
- Russignan A, Dal Collo G, Bagnato A, et al. Targeting the Endothelin-1 Receptors Curtails Tumor Growth and Angiogenesis in Multiple Myeloma. *Front Oncol*. 2020;10:600025.
- Hosen N, Matsunaga Y, Hasegawa K, et al. The activated conformation of integrin  $\beta(7)$  is a novel multiple myeloma-specific target for CAR T cell therapy. *Nat Med*. 2017;23:1436–1443.
- Kosti I, Jain N, Aran D, et al. Cross-tissue Analysis of Gene and Protein Expression in Normal and Cancer Tissues. *Sci Rep*. 2016;6:24799.
- Ferguson ID, Escobar BP, Tuomivaara ST, et al. Defining the cell surface proteomic landscape of multiple myeloma reveals immunotherapeutic strategies and biomarkers of drug resistance. *bioRxiv*. 2021:2021.01.17.427038.
- Di Meo F, Yu C, Cesarano A, et al. Mapping the high-risk multiple myeloma cell surface proteome identifies T-cell inhibitory receptors for immune targeting. *Blood*. 2021;138:265–265.
- Anderson GSF, Ballester-Beltran J, Giotopoulos G, et al. Unbiased cell surface proteomics identifies SEMA4A as an effective immunotherapy target for myeloma. *Blood*. 2022;139:2471–2482.